Self-assembled DNA nanostructures for distance-dependent multivalent ligand–protein binding

SHERRI RINKER†, YONGGANG KE†, YAN LIU*, RAHUL CHHABRA AND HAO YAN*

Department of Chemistry and Biochemistry, and Centre for Single Molecule Biophysics at the Biodesign Institute, Arizona State University, Tempe, Arizona 85287, USA

†These authors contributed equally to this work.

***e-mail: hao.yan@asu.edu; yan_liu@asu.edu**

Published online: 22 June 2008; doi:10.1038/nnano.2008.164

An important goal of nanotechnology is to assemble multiple molecules while controlling the spacing between them. Of particular interest is the phenomenon of multivalency, which is characterized by simultaneous binding of multiple ligands on one biological entity to multiple receptors on another[1]. Various approaches have been developed to engineer multivalency by linking multiple ligands together[2–4]. However, the effects of well-controlled inter-ligand distances on multivalency are less well understood. Recent progress in self-assembling DNA nanostructures with spatial and sequence addressability[5–12] has made deterministic positioning of different molecular species possible[8,11–13]. Here we show that distance-dependent multivalent binding effects can be systematically investigated by incorporating multiple-affinity ligands into DNA nanostructures with precise nanometre spatial control. Using atomic force microscopy, we demonstrate direct visualization of high-affinity bivalent ligands being used as pincers to capture and display protein molecules on a nanoarray. These results illustrate the potential of using designer DNA nanoscaffolds to engineer more complex and interactive biomolecular networks.

A multi-helix DNA tile was designed to display two different protein-binding short oligonucleotide sequences—aptamers[14]—with precise control over the distance between them. In the chosen model (Fig. 1) the two aptamers bind to thrombin (a coagulation protein involved as a key promotor in blood clotting). The aptamers we selected were chosen because they have been well characterized previously[15,16] and are known to bind to sites on almost opposite sides of the thrombin molecule[15,17,18]. Aptamer A (apt-A: 29-mer, 5′-AGT CCG TGG TAG GGC AGG TTG GGG TGA CT-3′) binds to the heparin-binding exosite[15], and aptamer B (apt-B: 15-mer, 5′-GGT TGG TGT GGT TGG-3′) binds primarily to the fibrinogen-recognition exosite[16]. We propose that, by varying the length of a rigid spacer, an optimal inter-aptamer distance will be achieved such that the two aptamers will act as a bivalent single molecular species that displays a stronger binding affinity to the protein than any one of the individual aptamers does alone.

The multi-helix DNA tile was designed and constructed from either a four-helix bundle (4HB) structure[19] or a five-helix bundle (5HB) structure (generated by narrowing an eight-helix bundle tile[19]) modified with the closed-loop aptamer sequences extending out from the ends of the helices (Fig. 1b). The spacing between the two aptamers can be controlled with subnanometre precision. For example, the 5HB DNA tile can provide 2, 3.5, 5.3 and 6.9 nm inter-aptamer distances. This was accomplished by integrating apt-A into helix 1 (the left-most helix) and moving apt-B from helix 2 to helix 5 (to the right). The relative axial orientation of the two aptamers was kept the same at all inter-aptamer distances.

We used gel-mobility shift assays to reveal the optimal spacing between apt-A and apt-B for bivalent binding. Owing to their smaller size, the 4HB-tile-based bivalent aptamers give a more obvious mobility shift during gel electrophoresis when bound with thrombin compared with that of the 5HB tiles. The 4HB tiles carrying aptamers at various spacings (2, 3.5 and 5.3 nm intervals) were incubated with and without thrombin (40 nM protein, [DNA tile]:[protein] = 1:2) before they were analysed using non-denaturing PAGE (see Methods and Supplementary Information).

The 4HB tile containing only apt-A on helix 1 (4HB-A1) and the 4HB tile containing only apt-B on helix 4 (4HB-B4) served as controls; both show no slower migrating band when incubated with thrombin (Fig. 2a, lanes 1–4) at this concentration. The dissociation constants (K_D) of these two aptamers with thrombin have been determined to be sub-nM or 75–100 nM (refs 15 and 16, respectively). Variations of K_D are seen in the literature depending on which method is used[15,16,20]. In the gel mobility assay, the binding complexes are not in equilibrium while migrating through the gel. Therefore the apparent dissociation constant K_D measured here is expected to be much larger than the solution K_D measured under equilibrium conditions. This can explain the observed low affinity of these two aptamers acting alone.

When tiles are incubated with thrombin and carry two differing aptamers at a distance of 2 nm (4HB-A1-B2), a very faint significantly slower migrating band can be seen, representing a small population of the DNA structure binding to thrombin (Fig. 2a, lanes 5 and 6). From the significant lagging position of the band, we propose that in this binding complex each thrombin molecule is sandwiched by two aptamers from two individual tiles[21]. At a distance of 3.5 nm (4HB-A1-B3), another distinct upper band appears closely above that of the DNA tiles.

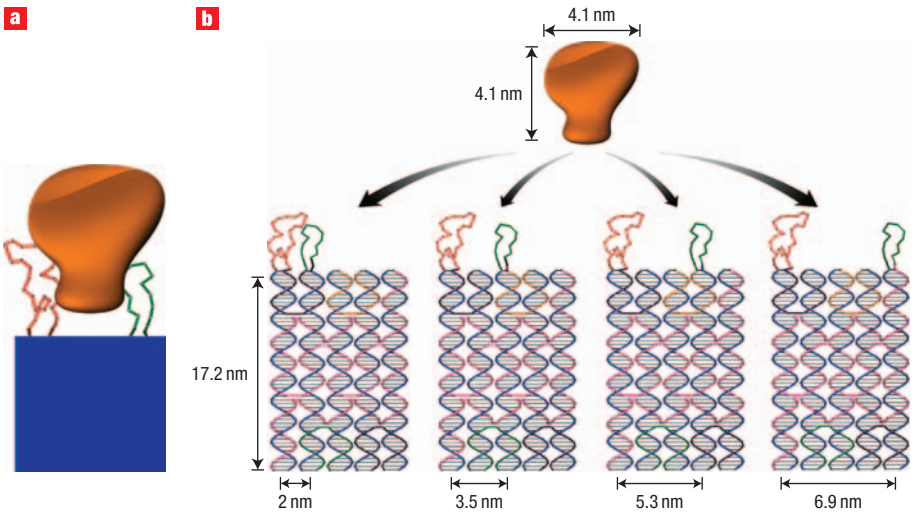

Figure 1 Schematics of the self-assembled divalent aptamers on a DNA tile for protein binding. a, Schematic showing a rigid DNA tile (blue) that can spatially separate two ligands (red and green) at a controlled distance, with each ligand attached to a different part of the target molecule (orange) for bivalent binding. **b**, Five-helix-bundle (5HB) DNA structure with apt-A (red) and apt-B (green) protruding out of the tile helices, separated by distances of 2, 3.5, 5.3, and 6.9 nm. The aptamer sequences were incorporated into the closed loops extending out of the ends of the helices. Apt-A is fixed on helix 1 and apt-B is moved between helix 2 and helix 5, generating the varying inter-aptamer distances but keeping the relative orientations constant. Numbering of the helices in the tile is read from left to right.

We propose that this band is due to the binding of one thrombin molecule by the two different aptamers on the same DNA tile (Fig. 2a, lanes 7 and 8), in other words, bivalent binding. It is estimated from the relative intensities of the upper and lower bands that ~25% of the structure is bound to thrombin. At a distance of 5.3 nm (4HB-A1-B4), the relative intensity of this band increases, and ~40% of the structure is bound with thrombin (Fig. 2a, lanes 9 and 10). Further, we used 5HB to generate a 6.9 nm spacing between the aptamers. The gel mobility shift assay (Fig. 2a lanes 11–14) showed a decreased binding at 6.9 nm spacing (5HB-A1-B5) compared to 5.3 nm spacing (5HB-A1-B4). Because the size of the thrombin protein is ~4 nm, we did not expect to see improved binding at any distances greater than 6.9 nm.

The percentage of protein-bound DNA tiles at the different spacings were estimated based on the gel shift assay in Fig. 2a, and plotted in Fig. 2b. It is noted that, for the same distance arrangements (5.3 nm), the thrombin-binding affinity of the bivalent aptamers on 5HB was slightly lower than that on 4HB. This difference is possibly due to the effect of the extra helix on the 5HB tile, which might limit the rotational freedom of the aptamer on the 4th helix. Overall, the inter-aptamer distance at 5.3 nm was determined to be optimal for bivalent binding (Fig. 2b).

As a control experiment to show that only hetero-aptamers can give such bivalent binding capability, we compared the binding of the tile containing two identical aptamers arranged at the same 5.3 nm distance, 4HB-A1-A4 and 4HB-B1-B4, with the tile containing two different aptamers (4HB-A1-B4). As shown in Fig. 2c, only the tile with the hetero-aptamers displayed an upper band when incubated with thrombin (lane 10). The homo-dimers did not show any significant binding, similar to the monomers. This result clearly indicated that the increased binding affinity is not caused by the increase in the number of aptamers per structure, but rather because of the type of aptamers that have a bivalent binding capability. We believe that the two hetero-aptamers act together as a pincer to grab the same thrombin molecule, each attaching to a different site on the protein. Such nano-pincers are able to bind thrombin tightly but can be made to release their ligands when triggered by an external chemical signal, that is, by adding the oligonucleotide complementary to the aptamer sequences (see Supplementary Information, Fig. S10).

One unique feature in our aptamer loop design is that we added four thymine bases (see Supplementary Information) at the end of the stems on both strands of the helix, thereby increasing their three-dimensional flexibility. Both aptamer sequences are known to have a stem/binding region, using only a few bases for contact with the surface of thrombin[15]. In order to find an optimal relative orientation of the two aptamers, we tried to rotate apt-B on the 4HB-A1-B4 by 90° and 180° by adding three or six base pairs to the stem, respectively. Both show a slight decrease in binding efficiency (see Supplementary Information, Fig. S1) in comparison to the original design of 4HB-A1-B4 (Fig. 2d); however, no obvious difference between these two structures was observed. We propose that the three-dimensional flexibility provided by the TTTT on the stems enables both aptamers to rotate in a limited range that can compensate for small changes in the centre-to-centre distances between the two aptamers so that bivalent binding efficiency can be maximized.

A rough estimate of the binding affinity of 4HB-A1-B4 to thrombin was obtained by titration of the thrombin concentration in the gel mobility shift assay (Fig. 2d lanes 1–8); a K_D of ~10 nM was obtained (see Supplementary Information and Methods). This is about a tenfold increase in affinity compared with that of the individual apt-A or apt-B on 4HB (4HB-A1 and 4HB-B4, in Fig. 2e lanes 1–14), which had a K_D estimated to be 20–50 nM and >50 nM, respectively. These titration results confirmed that the bivalent binding of the hetero-aptamers placed at an optimized distance can have a binding affinity better than the values for any of the monovalent binding arrangements.

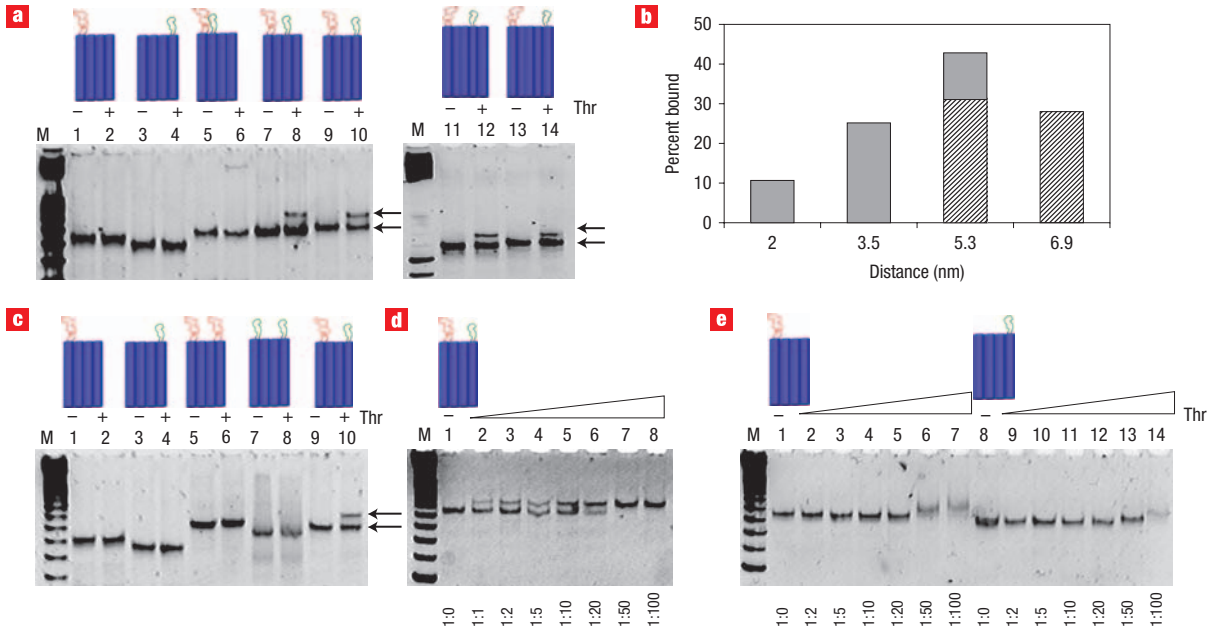

Figure 2 Gel-mobility shift assays. a, Non-denaturing (8% polyacrylamide) PAGE image of aptamers linked on the 4HB and 5HB tiles. Lane M corresponds to a 25 bp DNA marker. Lanes 1 to 14 correspond to 4HB-A1, 4HB-B4, 4HB-A1-B2 (2 nm), 4HB-A1-B3 (3.5 nm), 4HB-A1-B4 (5.3 nm), 5HB-A1-B4 (5.3 nm), and 5HB-A1-B5 (6.9 nm), each 20 nM without (–) and with (+) thrombin (40 nM), respectively. The lower band in each lane represents the unbound tiles and the upper band in lane 6, 8, 10, 12 and 14 represents the tile/thrombin complex. **b**, Dependence of protein binding on the inter-aptamer distance. Here 20 nM 4HB or 5HB tiles containing both apt-A and apt-B with varying inter-aptamer distances were incubated with 40 nM thrombin before they were loaded into the gel. The percentages of bound DNA tiles were estimated from the relative intensity of the bands in the gel image shown in panel **a**. The shaded and striped bars show data from the 4-HB and 5-HB tiles, respectively. **c**, The binding of thrombin to the 4HB tile-based aptamer structures carrying one aptamer or two of the same or different aptamers. All tiles with two aptamers have the same inter-aptamer distance at 5.3 nm. Lane M corresponds to a 25 bp DNA marker. Lanes 1 to 10 correspond to 4HB-A1, 4HB-B4, 4HB-A1-A4, 4HB-B1-B4, and 4HB-A1-B4 without (–) and with (+) thrombin (40 nM). An upper band is only observed in lane 10 with 4HB-A1-B4 (same as lane 10 in panel **a**). **d**, Titration experiment showing more DNA tiles (4HB-A1-B4, 1 nM) are bound to the protein with increasing concentrations of thrombin. Lane M corresponds to a 25 bp DNA ladder. From this gel a 10 nM apparent K_D is estimated for the bivalent binding of thrombin to the two aptamers linked by a DNA tile at a 5.3 nm distance. **e**, Titration experiment for 4HB-A1 (lanes 1–7) and 4HB-B4 (lanes 8–14). Lane M is a 25 bp DNA ladder. From this gel, the apparent K_D values for the two individual aptamers on the 4HB tile are estimated to be 20–50 nM and >50 nM, respectively.

We also attempted to adapt a solution-based method previously developed to measure the binding affinity of the aptamer to thrombin using a molecular aptamer beacon (MAB) (ref. 20). A K_D value for the 15-mer MAB has been reported as 5.2 nM (ref. 20). Using the same MAB, we observed effective displacement of the thrombin from the MAB by the 4HB-tile-based bivalence aptamer 4HB-A1-B4 (see Supplementary Information). From this displacement experiment, we estimated that the tile-based bivalent aptamer binds to thrombin ~50-fold more strongly than the 15-mer aptamer does and has a solution K_D of ~0.1 nM.

Atomic force microscopy (AFM) was also used to study the bivalent binding of these two aptamers at the single molecular level. Using the DNA origami method[9,11] we designed a rectangular-shaped DNA tile (Fig. 3a) of dimensions 60 x 90 nm. Stem-loops with apt-A and apt-B sequences were designed to protrude out of the plane of the DNA origami tile. We put two lines of each aptamer (for a total of four lines of aptamer probes) on the DNA origami tile, with a distance of ~20.7 nm and ~5.8 nm between the neighboring lines of apt-A and apt-B, and an intra-line distance of ~12 nm for the same aptamer. Based on the estimated K_D values, when we add a 1:4 ratio of thrombin to the total number of aptamers, no or low binding is expected on the lines that are further apart, but stronger binding is expected on the bivalent dual-aptamer lines (marked as A+B in Fig. 3a). A group of six closely placed dumb-bell loops that provide a height contrast under AFM imaging was positioned in one corner of the tile as a topographic index reference to unambiguously determine the relative positions of each aptamer line.

To rule out the possibility of positional effects due to electrostatic repulsion between the probes and the DNA scaffold[12], the positions of the dual-aptamer lines were switched from close to one side of the tile to the middle on another DNA origami tile (Fig. 3b). AFM images (Fig. 3c,d) showed that thrombin preferred to bind to the dual-aptamer lines on both DNA origami tiles. Individual protein molecules can be distinctly detected. We counted the number of protein molecules bound to each aptamer line (Fig. 3e,f). The dual-aptamer line shows an approximately tenfold better protein binding than the single aptamer lines, consistent with the gel assay results.

Whitesides and colleagues[1] have previously pointed out that "the more conformationally rigid the polyvalent entity is, the more likely it is that even small spatial mismatches between the ligand and its receptor will result in enthalpically diminished binding (unless the geometric fit between ligand and receptor is accurate at a picometre scale, which is exceedingly rare)." Here we have a rigid scaffold that has spatial accuracy at the nanometre scale in which such diminished binding is unavoidable. Limited conformational flexibility will help to

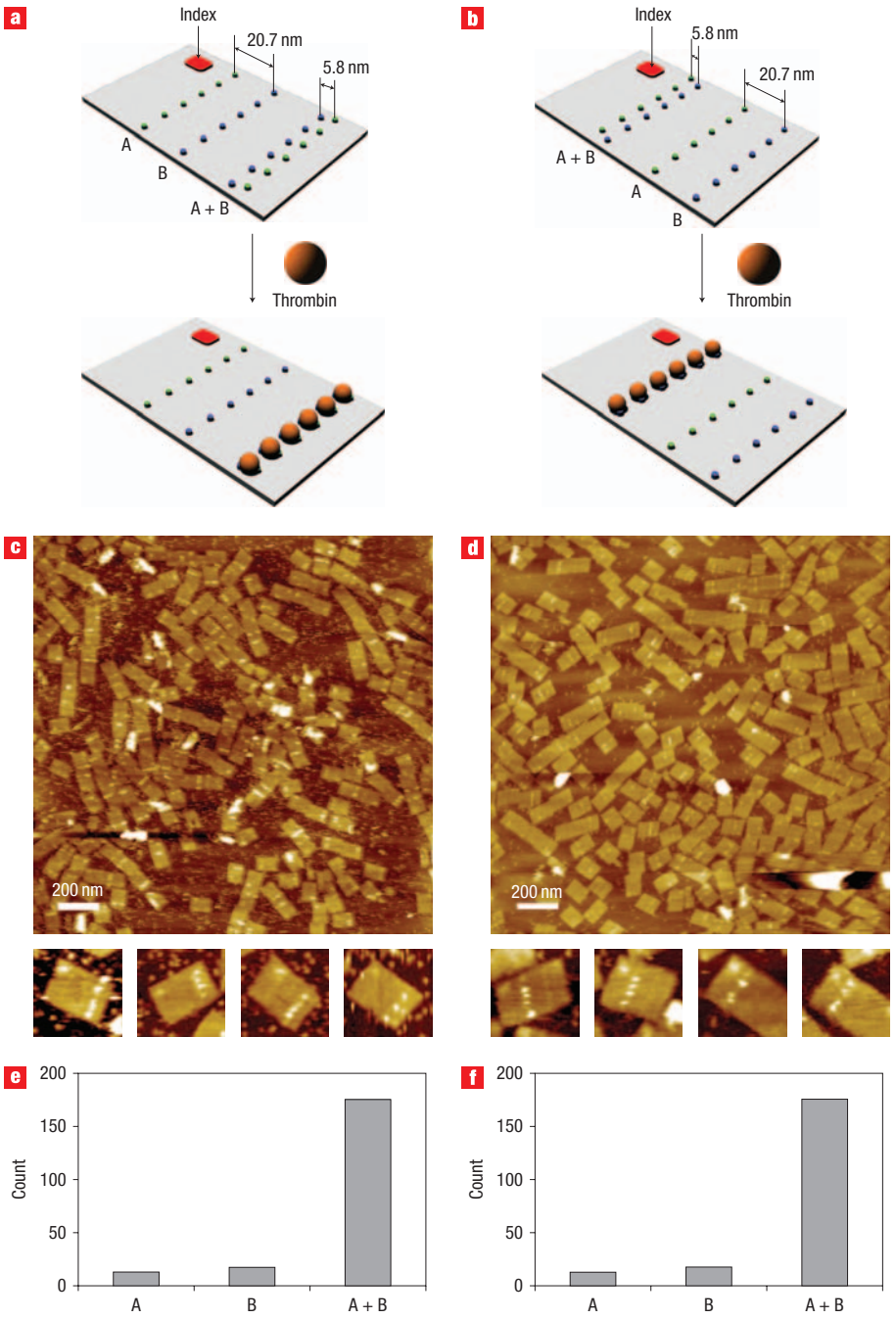

Figure 3 Evaluation of bivalent binding by AFM. a,**b**, Schematic drawings of two rectangular-shaped DNA origami tiles containing two lines of apt-A (green dots) and two lines of apt-B thrombin (blue dots). The neighboring lines of apt-A and apt-B are ~20.7 nm (marked line A and line B) and ~5.8 nm (line A+B) apart. We call the closely spaced lines the dual-aptamer line. An index is also included that helps to verify the positions of the lines in the AFM images. **c**,**d**, AFM height images of the DNA origami tiles (10 nM) with 60 nM thrombin, corresponding to **a** and **b**, respectively. Enlarged images are 150 × 150 nm. **e**,**f**, Charts of numbers of proteins binding on each aptamer line (observed from 60 arrays corresponding to **a** and **b**, respectively). Bar A represents the number of proteins on the line of apt-A, bar B represents the number of proteins on the line of apt-B, and bar A+B represents the number of proteins on the bivalent dual-aptamer line.

compensate for small spatial mismatches at a cost of certain entropy loss. Nevertheless, the trend of distance-dependent effect on multivalent binding observed at this spatial resolution is still very interesting.

This study also represents the first example of using the spatial addressability of self-assembled DNA nanoscaffolds to control multi-component biomolecular interactions and to visualize such interactions at a single-molecule level. In addition to aptamers, it may be possible to position small peptides[22], subdomains and cofactors of enzymes, or carbohydrate molecules into two-dimensional and three-dimensional spatially controlled networks to obtain multivalent behaviour, which may be used to probe

steric constraints, ionic interactions and hydrophobic interactions. It may also be possible to use addressable DNA nanoscaffolds[5–10,12,13,23] to position motor proteins at a particular inter-molecular distance to display complex motor behaviours on a well-defined nanoscale landscape, generated, for example, by modifying the staple strands of the origami at different locations.

METHODS

THROMBIN BINDING AND GEL-SHIFT ASSAY

All oligonucleotides were synthesized by Integrated DNA Technology Incorporated and purified by 10% denaturing polyacrylamide gel electrophoresis (PAGE). (See Supplementary Information for a complete list of oligonucleotides used.) The concentration of each strand was measured by OD_{260}. Each individual tile was assembled by mixing each strand to a final concentration of 1.0 μM per strand, and annealed using an Eppendorf thermocycler starting at 90 °C and decreased by 0.4 °C per minute to 24 °C. The tiles were further diluted for thrombin binding and gel-shift assays. Human α-thrombin was purchased from Haematologic Technologies. The concentration was estimated at OD_{280}. All buffers used in the experiments contained 100 mM Tris, 50 mM acetic acid, 5 mM EDTA, and 12.5 mM magnesium acetate. 4HB and appropriate aptamers were incubated with specified amounts of thrombin for 1 h at room temperature. Non-denaturing PAGE was run on Amersham Ruby-600 at a constant 200 V for 4 h (for 8% gels) or 12 h (for 6% gels) and stained with SybrGold (Invitrogen, 1×dye in 100 ml water) or SybrGreen (Invitrogen, 1×dye in 100 ml water). Gels were imaged with the Epichem3 Darkroom gel documentation system (UVP BioImaging Systems), and band intensity was densitometrically measured with Labworks software or with Image J (http://rsb.info.nih.gov/ij/).

AFM IMAGING

Rectangular-shaped DNA origami tiles were assembled according to Rothemund's method[9]. Helper strands modified with aptamer sequences were purified using denaturing PAGE and mixed with the viral DNA and the unmodified helper strands at a molar ratio of 1:1:5. Each array contained 24 thrombin-binding aptamers (12 apt-A and 12 apt-B). Arrays (10 nM) were mixed with thrombin (60 nM, or 1:1 ratio of the dual aptamer to thrombin) for 1 h before imaging. The sample (2 μl) was deposited onto a freshly cleaved mica cell (Ted Pella) and left to adsorb for 3 min. 1×TAE/Mg buffer (400 μl) was added to the liquid cell and the sample was scanned in a tapping mode under fluid on a Pico-Plus AFM (Molecular Imaging, Agilent Technologies) with NP-S tips (Veeco). Low concentrations of protein were also imaged (see Supplementary Information, Fig. S5).

Received 3 December 2007; accepted 19 May 2008; published 22 June 2008.

References

1. Mammen, M., Choi, S. K. & Whitesides, G. M. Polyvalent interactions in biological systems: implications for design and use of multivalent ligands and inhibitors. *Angew. Chem. Int. Ed.* **37,** 2755–2794 (1998).
2. Di Giusto, D. A. & King, G. C. Construction, stability, and activity of multivalent circular anticoagulant aptamers. *J. Biol. Chem.* **279,** 46483–46489 (2004).
3. Fredriksson, S. *et al.* Protein detection using proximity-dependent DNA ligation assays. *Nat. Biotechnol.* **20,** 473–477 (2002).
4. Pei, R. *et al.* Behaviour of polycatalytic assemblies in a substrate-displaying matrix. *J. Am. Chem. Soc.* **128,** 12693–12699 (2006).
5. Rothemund, P. W. K., Papadakis, N. & Winfree, E. Algorithmic self-assembly of DNA sierpinski triangles. *PloS. Biol.* **2,** 2041–2053 (2004).
6. Lund, K., Liu, Y., Lindsay, S. & Yan, H. Self-assembling a molecular pegboard. *J. Am. Chem. Soc.* **127,** 17606–17607 (2005).
7. Liu, Y., Ke, Y. G. & Yan, H. Self-assembly of symmetric finite-size DNA nanoarrays. *J. Am. Chem. Soc.* **127,** 17140–17141 (2005).
8. Park, S. H. *et al.* Finite-size, fully addressable DNA tile lattices formed by hierarchical assembly procedures. *Angew. Chem. Int. Ed.* **45,** 735–739 (2006).
9. Rothemund, P. W. K. Folding DNA to create nanoscale shapes and patterns. *Nature* **440,** 297–302 (2006).
10. Pistol, C. & Dwyer, C. Scalable, low-cost, hierarchical assembly of programmable DNA nanostructures. *Nanotechnology* **18,** 125305 (2007).
11. Chhabra, R. *et al.* Spatially addressable multiprotein nanoarrays templated by aptamer-tagged DNA nanoarchitectures. *J. Am. Chem. Soc.* **129,** 10304–10305 (2007).
12. Ke, Y., Lindsay, S., Yung, C., Liu, Y. & Yan, H. Self-assembled water soluble nucleic acid probe tiles for label-free RNA hybridization assays. *Science* **319,** 180–183 (2008).
13. Zheng, J. W. *et al.* Two-dimensional nanoparticle arrays show the organizational power of robust DNA motifs. *Nano Lett.* **6,** 1502–1504 (2006).
14. Nimjee, S. M., Rusconi, C. P. & Sullenger, B. A. Aptamers: an emerging class of therapeutics. *Annu. Rev. Med.* **56,** 555–583 (2005).
15. Tasset, D. M., Kubik, M. F. & Steiner, W. Oligonucleotide inhibitors of human thrombin that bind distinct epitopes. *J. Mol. Biol.* **272,** 688–698 (1997).
16. Bock, L. C., Griffin, L. C., Latham, J. A., Vermaas, E. H. & Toole, J. J. Selection of single-stranded-DNA molecules that bind and inhibit human thrombin. *Nature* **355,** 564–566 (1992).
17. Padmanabhan, K., Padmanabhan, K. P., Ferrara, J. D., Sadler, J. E. & Tulinsky, A. The structure of alpha-thrombin inhibited by a 15-mer single-stranded-DNA aptamer. *J. Biol. Chem.* **268,** 17651–17654 (1993).
18. Stubbs, M. T. & Bode, W. The clot thickens: clues provided by thrombin structure. *Trends Biochem. Sci.* **20,** 23–28 (1995).
19. Ke, Y., Liu, Y., Zhang, J. & Yan, H. A study of DNA tube formation mechanisms using 4-, 8-, and 12-helix DNA nanostructures. *J. Am. Chem. Soc.* **128,** 4414–4421 (2006).
20. Li, J., Fang, X. & Tan, W. Molecular aptamer beacons for real-time protein recognition. *Biochem. Biophys. Res. Comm.* **292,** 31–40 (2002).
21. Liu, Y., Lin, C., Li, H. & Yan, H. Aptamer-directed self-assembly of protein arrays on a DNA nanostructure. *Angew. Chem. Int. Ed.* **44,** 4333–4338 (2005).
22. Williams, B. A. R., Lund, K., Liu, Y., Yan, H. & Chaput, J. C. Self-assembled peptide nanoarrays: an approach to studying protein–protein interactions. *Angew. Chem. Int. Ed.* **46,** 3051–3054 (2007).
23. Tumpane, J. *et al.* Triplex addressability as a basis for functional DNA nanostructures. *Nano Lett.* **7,** 3832–3839 (2007).

Supplementary Information accompanies this paper at www.nature.com/naturenanotechnology.

Acknowledgements

This work was derived from a discussion of the synthetic antibody project with S.A. Johnston at the Biodesign Institute, Arizona State University. We also thank S. Lindsay, C. Diehnelt and Dong-Kyun Seo for helpful discussions. S.R. was partly supported by the Technology and Research Initiative Fund from Arizona State University to S.A. Johnston. This work was partly supported by grants from the National Science Foundation, the National Institute of Health, the Air Force Office of Scientific Research and the Office of Naval Research to Hao Yan and TRIF funds from Arizona State University to Hao Yan and Yan Liu.

Author contributions

H.Y. and Y.L conceived the project. H.Y., Y.L, S.R. and Y.K. designed the experiments. S.R., Y.K. and R.C. performed the experiments. H.Y., Y.L., S.R. and Y.K. analysed the data. H.Y., Y.L. and S.R. co-wrote the paper. All authors discussed the results and commented on the manuscript.

Author information

Reprints and permission information is available online at http://npg.nature.com/reprintsandpermissions/. Correspondence and requests for materials should be addressed to H.Y and Y.L.